International Journal of Engineering and Advanced Technology (IJEAT)
ISSN: 2249-8958 (Online), Volume-9 Issue-3, February 2020

Free Vibration Response of Four-Parameter Functionally Graded Thick Spherical Shell Formulation on Higher-Order Shear Deformation Theory

Raparthi Srilakshmi, Ch. Ratnam, Chandra Mouli Badiganti

***Abstract:** This paper emphasizes on the free vibration (FV) responses of functionally graded thick spherical shell in rectangular form using traditional mathematical formulation on finite element method and governed by Higher order shear deformation theory (HOSDT). A functionally graded spherical shell made up of metal-rich on the top surface and in contrast, base surface of the model is ceramic-rich. The FG volume fraction of four-parameter power-law material constituents assumed in the thickness direction. To highlight the potential for the current method, convergence studies, and validation tests performed to establish the stability and accuracy attained by the current approach. The parametric studies presented to scrutinize the influence of choice of four parameters employed through power-law distribution. The eminence effect of spherical shell geometrical properties, and different types of support conditions, skew angle on the FV behavior of non-dimensional frequency responses examined in detail.*

***Keyword:** Free vibration, HSDT, Finite element method, Spherical shell.*

I. INTRODUCTION

The continuous evaluation of develop materials and to optimize the structural design have received significant attention in many engineering areas and manufacturing industries. FGMs are a structurally advanced new class of composites. The concept originated in the 1980s in Japan. FGMs continuous gradation behavior of material composition (metal and ceramic) and microstructure. FGMs preferred in many sectors because of their mechanical and heat-shielding characteristics while maintaining structural integrity and reducing stress concentrations. Many research works contributed to bending and buckling analysis. The vibration behavior of shells plays a crucial role in design aerospace equipment, spacecraft, rockets, missiles, containers, hydraulic structures, submarines, ships, storage tanks.

Revised Manuscript Received on February 05, 2020.
* Correspondence Author
Raparthi Srilakshmi*, Department of Mechanical Engineering, Andhra University, Visakhapatnam, India. Email: srilakshmi053@gmail.com
Ch.Ratnam, Department of Mechanical Engineering, Andhra University, Visakhapatnam, India. Email: chratnam@gmail.com
Chandra Mouli Badiganti, Department of Mechanical Engineering, RISE Group of Institutions, Ongole, India. Email: badiganti1@gmail.com

Revised Manuscript Received on February 05, 2020.
* Correspondence Author

Loy et al. [1] examined the vibration of cylindrical with FGMs constituents with- general boundary conditions. The analysis considered based-on Love's Shell theory and Rayleigh-Ritz's method. A similar approach followed Pradhan et al. [2] studied FG Cylindrical Shells under different boundary conditions formulation on classical plate theory. Reddy [3] presented an analysis of Functionally graded plates. Ng et al. [4] introduced the dynamic stability analysis of FG shells under harmonic axial loading and Bolotin's approximation. K. M. Liew et al. [5] studied a three-dimensional vibration analysis of spherical shells panel subjected to various boundary conditions employing the P-Ritz method.

J.N. Reddy and Z.Q. Cheng [6] studied a spherical shallow shell in polygonal planform resting on a Winkler Pasternak elastic foundation. Hu et al. [7] studied the natural frequencies of rotating twisted and open conical shells. E. Artioli and Viola [8] presented the FV analysis of spherical caps using the Generalized Differential Quadrature (GDQ) procedure and the FEM approach. Arciniega and J.N. Reddy [9] described, Nonlinear analysis for functionally graded shells. The formulation is on the first-order shear deformation theory (FSDT) with seven independent parameters.

Zhao et al. [10] analyzed the FV of functionally graded shells using the element-free KP-Ritz method.F. Tornabene and E. Viola [11], [12] investigated the dynamic behavior of vibration analysis of hemispherical domes and spherical shell panels using FSDT. Later on, the same authors developed a 2-D solution for free vibrations of parabolic shells using a GDQ, and the FSDT is used to analyze the above moderately thick structural elements. Numerical solutions with the ones obtained using commercial programs such as Abaqus, Ansys, Femap/Nastran, Straus, Pro/Mechanica used. F. Tornabene [13] investigated based on the FSDT. Dynamic behavior of moderately thick FG conical, cylindrical shells, and annular plates with two different power-law distributions presented. Tornabene et al. [14]– [16] extended the GDQ procedure for the FV analysis of FG doubly-curved panels and shells of revolution with classical boundary conditions.

M.H.yas and B. Sobhani Aragh [17] studied three-dimensional analysis for the thermoelastic response of functionally graded fiber-reinforced cylindrical panel.

Amabili and J.N. reddy [18] studied higher-order deformation nonlinear theory for the large amplitude of forced vibration of laminated doubly curved shells. Mohammad Talha and B.N Singh [19] studied static response and FV analysis of FGM plates using higher order shear deformation theory and conjunction with finite element method.

Shen and Z.X. Wang [20] described based on HSDT, comparison studies of two kinds of micromechanics models, namely Voigt's and Mori-Tanaka models for vibration analysis of FG plates. Neves A.M.A et al. [21] presented with FV problems of FG spherical as well as cylindrical shell panels with all edges clamped or simply supported. The analysis is performed by radial basis functions collocation, according to a HSDT that accounts for through-the-thickness deformation. Discretization method-based on the FSDT.

V. R. Kar and S. K. Panda [22]. investigated the vibration and thermal buckling characteristics of FG single/double curved panels under linear and nonlinear behaviors temperatures fields are studied. Kumar et al. [23] developed for FV analysis of laminated composite skew cylindrical shells. A C_0 finite element formulation based on using HSDT.

C. Zhang et al. [24] presented the improved Fourier series method based on Hamilton's principle to investigate the vibration characteristics of circular cylindrical double-shell structures with different boundary conditions. Devesh Punera and Tarun Kant [25] developed FV of FG open cylindrical shells based on several refined higher-order displacement models. Mouli and Ramji Koona [26]-[28] examined the influence of different parameters on the FV behavior of FG Skew shallow curved panels.

In the present work focused on the FV characteristics of FGM rectangular spherical shell. The formulation based on Higher-order deformation theory conjunction with the finite-element method. The comprehensive parametric studies carried out to examine the influence of power-law distribution and Choice of four parameters on material composition in terms of volume fraction constituents. and the significance of Geometric parameters is that the shell aspect ratio, thickness ratio, and curvature ratio. and the impact of different boundary conditions, skew angle, on the non-dimensional frequency responses, are studied.

II. FGM MATERIAL PROPERTIES AND FOUR-PARAMETER POWER-LAW DISTRIBUTION PARAMETERS

In this part, the variation of volume fraction through the different values of power-law exponent and choice of distribution parameters with classic, with reference surface to the shell (Symmetric) and without reference surface (asymmetric) volume fraction profiles illustrated. The material properties of the FG spherical shell are assumed to vary throughout the thickness, where ϑ_m and ϑ_c are the volume fractions of metal and ceramic. Similarly, in which subscripts c and m represent the ceramic and metal constituents, as in (1a), (1b), and (1c) mechanical properties are Young's modulus E(ξ), density(ξ), and poisons ratio(ν) vary continuously to achieve smooth gradation of material phase through the spatial direction (ξ) expressed in the form of a linear combination. The sum of the volume fraction of the constituent materials should be equal to one, as in (2).

$$\mathrm{E}(\xi) = (E_c - E_m)\vartheta_c + \vartheta_m \qquad (1a)$$

$$\rho(\xi) = (\rho_c - \rho_m)\vartheta_c + \rho_m \qquad (1b)$$

$$\nu(\xi) = (\vartheta_c - \vartheta_m)\vartheta_c + \vartheta_m \qquad (1c)$$

$$\vartheta_c + \vartheta_m = 1 \qquad (2)$$

According to the following power-law function as in (3) Where φ is the power-law exponent varying as 0 ≤ φ ≤ ∞, and the distribution parameters u, v, w and different values of power law exponent generates material variation profiles through the thickness direction in terms of volume fraction. For example, FG constituents of the shell thickness demonstrated through four parameter power law distribution. the material distribution in the FGM shell is continuously varied, such that the bottom surface (-h/2) of the structure is pure ceramic. In contrast, the top surface (+h/2) pure metal, by setting u = 1 and v = 0, w=0, as in (3).

$$\mathrm{FGM}_{(u/v/w/\varphi)}: \vartheta_C = \left(1 - u\left(\frac{1}{2}+\frac{\xi}{h}\right) + \mathrm{v}\left(\frac{1}{2}+\frac{\xi}{h}\right)^{w}\right)^{\varphi} \qquad (3)$$

Fig.1 shows the classic volume fraction profiles, power-law distributions are considered for the volume fraction of the ceramic. The first distribution FGM (u=1, v=0/w=1/φ), the material composition is continuously varied, such that the bottom surface of ξ/h=-0.5 of the shell's ceramic-rich. In contrast, the top surface (ξ/h=0.5) is metal-rich.

Fig.2 shows the significance of the various power-law distribution of patterns by modifying the parameters u, v, w, and φ for the given constituents of volume fraction.by varying the power law exponent (φ) and symmetric respect to the reference surface (ξ/h=0) of the shell.by setting the first four parameter power law distribution FGM (u=1,v=1 and w=3).

Fig.3 illustrate profiles are not symmetric with respect to the reference surface (ξ/h=0) of the shell. asymmetric profiles obtained by setting FGM (u=1, v=1, w=5/φ).

Figs.4-6. depicts varying the parameters u, v, w. These material profiles characterized by the fact that one of the shells surfaces the top or bottom surface presents a composed of two constituents. For example, by setting the values as in (3) and the power-law distribution is FGM (u=1, v=0.4, w=3) and different quantity values of the power-law exponent. From the design point of view, it is essential to know the top surface is of the shell ξ/h=0.5 is ceramic or metal. If the bottom surface ξ/h=-0.5 is metal or ceramic- rich. One of these surfaces presents a mixture of two constituents. It is worth noting that types four-parameter power-law distributions as enunciated by F. Tornabene [13]-[16], and the author provided more detailed descriptions about the material variation profile of FGMs.

The primary purpose of this section The Voigt's rule is employed to estimate the ceramic volume fraction. The four-parameter power-law distribution affects the desired volume fraction of the material on the top and bottom surface of the structure.

Thus, FGM material properties of layers change continuously and smoothly in the thickness direction. The influence of the choice of four material parameters u, v, w, φ, and to study the variation of the volume fraction of the material constituents and effects of various forms of classic, symmetric and asymmetric material pattern profiles which change the mechanical behavior of a structure.

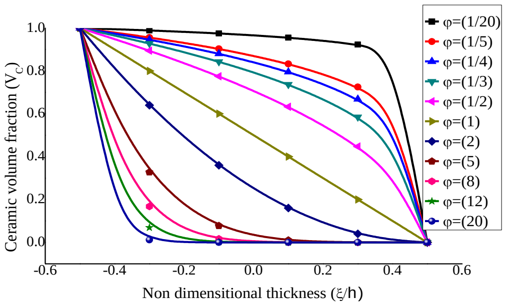

Fig.1. FGM (u=1/v=0/w=1/φ)

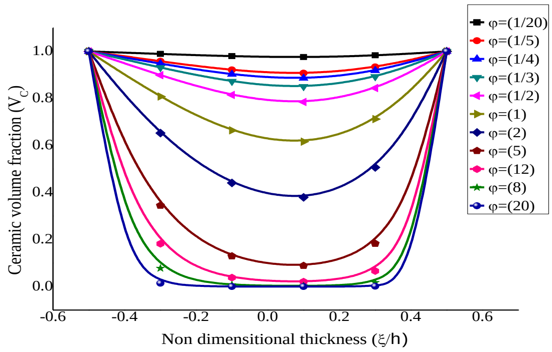

Fig. 1. FGM (u=1/v=1/w=3/φ)

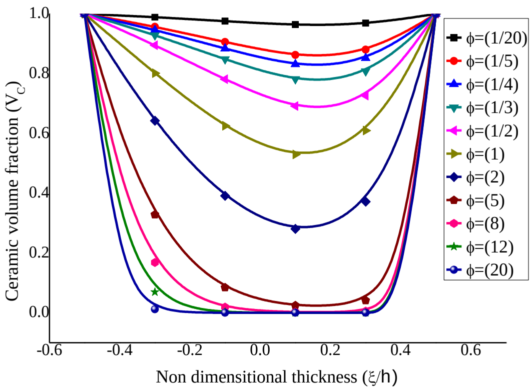

Fig.3.FGM (u=1/v=1/w=5/φ)

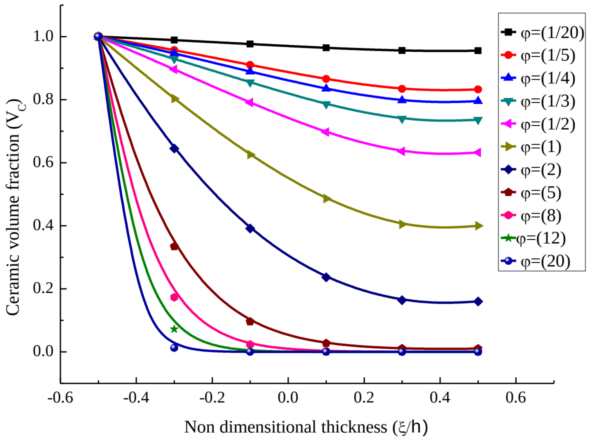

Fig. 2. FGM (u=1/v=0.4/w=3/φ)

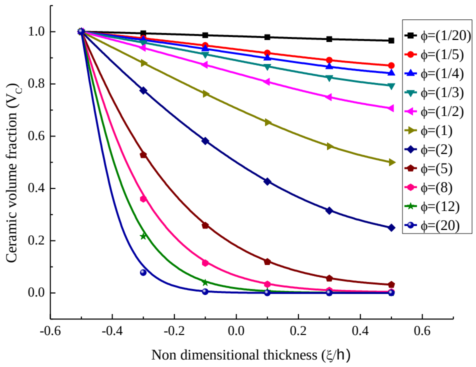

Fig.3. FGM (u=0.6/v=0.1/w=0.4/φ)

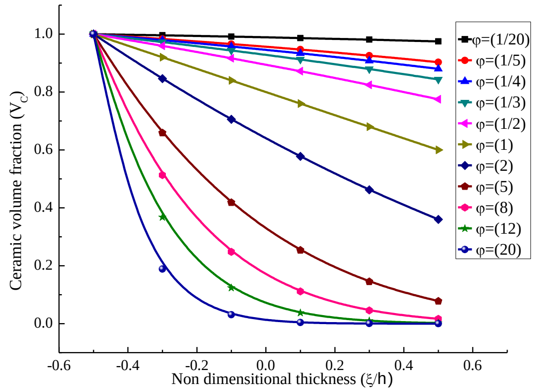

Fig.6. FGM (u=0.4/v=0/w=1/φ)

Fig. 1-6. Variation of ceramic volume fraction (ϑ_c)through the FG structure thickness(ξ) for different values of three parameters u, v, w, and φ

III. FRAMEWORK OF GOVERNING EQUATIONS

3.1 Kinematic Paradigm and numerical procedure

In this framework, the formulation procedure for governing equations obtained by a general shallow curved spherical shell is represented by a, b, and thickness h, in x, y directions, as shown in Fig.7. Here, Rx and Ry are the radii of curvature along x and y direction, respectively. The TSDT mid-plane kinematics model utilized to define the global displacements (χ,λ,ψ,) at any point in terms of mid-plane displacements (χ_0, λ_0, ψ_0),

rotations (θ_x, θ_y) and higher-order ($\chi_0^*, \lambda_0^*, \theta_x^*, \theta_y^*$) terms, as per Pandya & Kant, [30].

$$\left.\begin{aligned} \chi &= \chi_0 + \xi\theta_x + \xi^2\chi_0^* + \xi^3\theta_x^* \\ \lambda &= \lambda_0 + \xi\theta_y + \xi^2\lambda_0^* + \xi^3\theta_y^* \\ \psi &= \psi_0 \end{aligned}\right\} \tag{4}$$

This kinematic model, (5) can be rewritten in the matrix form as in (5)

$$\{\delta\} = [F]\{\delta_0\} \tag{5}$$

where,$\{\delta\} = \lfloor \chi \quad \lambda \quad \psi \rfloor^T$and $\{\delta_0\} = \lfloor \chi_0 \quad \lambda_0 \quad \psi_0 \quad \theta_x \quad \theta_y \quad \chi_0^* \quad \lambda_0^* \quad \theta_x^* \quad \theta_y^* \rfloor^T$are the global and mid-plane displacement vectors. $[F]$ contains the thickness coordinate functions, as expressed here in (6)

$$[F] = \begin{bmatrix} 1 & 0 & 0 & \xi & 0 & \xi^2 & 0 & \xi^3 & 0 \\ 0 & 1 & 0 & 0 & \xi & 0 & \xi^2 & 0 & \xi^3 \\ 0 & 0 & 1 & 0 & 0 & 0 & 0 & 0 & 0 \end{bmatrix} \tag{6}$$

The shallow curved shell is shown in Fig.7(ii) with sides a and b. To constraint the oblique edges, the local displacement vector is required to transform to global via transformation matrix [F and expressed in cosine (l) and sine (m) terms. The displacement transformation revealed as

$$\begin{Bmatrix} \chi_0 \\ \lambda_0 \\ \psi_0 \\ \theta_x \\ \theta_y \\ \chi_0^* \\ \lambda_0^* \\ \theta_x^* \\ \theta_y^* \end{Bmatrix} = \begin{bmatrix} l & -m & 0 & 0 & 0 & 0 & 0 & 0 & 0 \\ m & l & 0 & 0 & 0 & 0 & 0 & 0 & 0 \\ 0 & 0 & 1 & 0 & 0 & 0 & 0 & 0 & 0 \\ 0 & 0 & 0 & l & -m & 0 & 0 & 0 & 0 \\ 0 & 0 & 0 & m & l & 0 & 0 & 0 & 0 \\ 0 & 0 & 0 & 0 & 0 & l & -m & 0 & 0 \\ 0 & 0 & 0 & 0 & 0 & m & l & 0 & 0 \\ 0 & 0 & 0 & 0 & 0 & 0 & 0 & l & -m \\ 0 & 0 & 0 & 0 & 0 & 0 & 0 & m & l \end{bmatrix} \begin{Bmatrix} \chi_0' \\ \lambda_0' \\ \psi_0' \\ \theta_x' \\ \theta_y' \\ \chi_0^{*\prime} \\ \lambda_0^{*\prime} \\ \theta_x^{*\prime} \\ \theta_y^{*\prime} \end{Bmatrix} \tag{7}$$

(7) can also be written as

$$\{\Omega_0\} = [F]\{\Omega_0'\} \tag{8}$$

where, $\{\Omega_0'\}$ is the displacement field defined in the local coordinates.

The strain-displacement equation for any general shallow thick plate can be written as (Kar and Panda, [22])

$$\begin{Bmatrix} \varepsilon_{xx} \\ \varepsilon_{yy} \\ \gamma_{xy} \\ \gamma_{xz} \\ \gamma_{yz} \end{Bmatrix} = \begin{Bmatrix} \frac{\partial\chi}{\partial x} + \frac{\psi}{R_x} \\ \frac{\partial\lambda}{\partial y} + \frac{\psi}{R_y} \\ \frac{\partial\chi}{\partial y} + \frac{\partial\lambda}{\partial x} \\ \frac{\partial\chi}{\partial z} + \frac{\partial\psi}{\partial x} - \frac{\chi}{R_x} \\ \frac{\partial\lambda}{\partial z} + \frac{\partial\psi}{\partial y} - \frac{\lambda}{R_y} \end{Bmatrix} \tag{9}$$

By imposing the displacement terms (4) in the strain-displacement as in (9), the global strain tensor can be modified as

$$\begin{Bmatrix} \varepsilon_{xx} \\ \varepsilon_{yy} \\ \gamma_{xy} \\ \gamma_{xz} \\ \gamma_{yz} \end{Bmatrix} = \begin{Bmatrix} \varepsilon_x{}^0 \\ \varepsilon_y{}^0 \\ \varepsilon_{xy}{}^0 \\ \varepsilon_{xz}{}^0 \\ \varepsilon_{yz}{}^0 \end{Bmatrix} + \xi \begin{Bmatrix} k_x{}^1 \\ k_y{}^1 \\ k_{xy}{}^1 \\ k_{xz}{}^1 \\ k_{yz}{}^1 \end{Bmatrix} + \xi^2 \begin{Bmatrix} k_x{}^2 \\ k_y{}^2 \\ k_{xy}{}^2 \\ k_{xz}{}^2 \\ k_{yz}{}^2 \end{Bmatrix} + \xi^3 \begin{Bmatrix} k_x{}^3 \\ k_y{}^3 \\ k_{xy}{}^3 \\ k_{xz}{}^3 \\ k_{yz}{}^3 \end{Bmatrix} \tag{10}$$

$$\varepsilon = \varepsilon^0 + \xi k^1 + \xi^2 k^2 + \xi^3 k^3 \tag{11}$$

where, ε^0, k^1, k^2 and k^3 are the mid-plane strain, curvature and higher-order terms respectively as per Kar and Panda [22].

(11) can be again rearranged as

$$\{\varepsilon\} = [F]\{\bar{\varepsilon}\} \tag{12}$$

where, $\{\bar{\varepsilon}\} = \lfloor \varepsilon^0 \quad k^1 \quad k^2 \quad k^3 \rfloor^T$ is the mid-plane strain, and $F = [I \quad \xi I \quad \xi^2 I \quad \xi^3 I]$ is the thickness-coordinate matrix, in which I is the unit matrix of size 5×5.

3.2 Finite Element Approximations

In this section, the present FG shallow spherical panel is discretized based on a finite element modeling using a nine-node isoperimetric element with eighty-one degrees-of the displacements defined in the mid-plane can in a nodal form as

$$\{\Omega_0\} = \sum_{i=1}^{9} N_i \{\Omega_{0_i}\} \tag{13}$$

where, $\{\Omega_{0_i}\}$ and N_i are the nodal displacement vector and the approximation function at ith node (Cook et al. [29]). Now, the total and geometric mid-plane strain vectors can be expressed as in (13) as

$$\{\bar{\varepsilon}\} = [B]\{\Omega_{0_i}\} \text{ and } \{\bar{\varepsilon}_G\} = [B_G]\{\Omega_{0_i}\} \tag{14}$$

where, $[B]$ and $[B_G]$ are the differential operators of the total and geometrical mid-plane strains respectively. By imposing (12)-(15) in the above governing equation, the equilibrium equation of the vibrated FG shallow shell panel is achieved and expressed in global form, as

$$([K] - [K_G] - \omega^2[M])\Delta = 0 \tag{15}$$

where, $[M] = [N]^T [m][N]$ is the global mass matrix,

$[K] = [B]^T [D][B]$ is the global stiffness matrix,

$[K_G] = [B_G]^T [D_G][B_G]$ is the geometric stiffness matrix and ω and Δ are the natural frequency and eigenvalue type the corresponding eigen vectors.

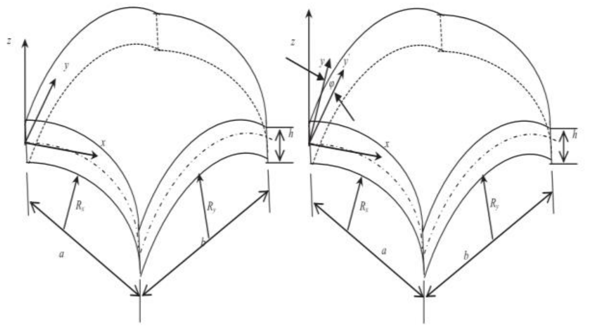

Fig. 7.(i) spherical curved shell form (ii) spherical curved shell skew form

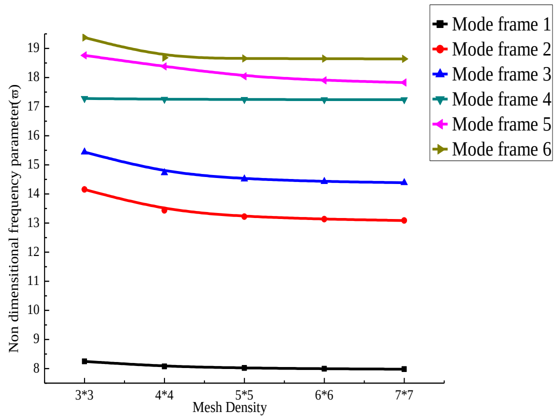

Fig. 8. Dimensionless frequency parameter SSSS

IV. RESULTS AND DISCUSSION

The theoretical model is developed in the present study using the HSDT and FG spherical shells under FV analysis. Material Properties play a vital role in determining the response of natural frequencies of the FG Spherical shell. Table I. shows the material properties of FGM constituents. It should be that the

non-dimensional excitation frequency parameter defined. The results presented in Table II-XII are shown based on the dimensionless natural frequency, according to, as in (16).

$$\left(\overline{\omega} = \omega(a^2/h)\sqrt{\rho_c/E_c}\right) \tag{16}$$

Table I. Material properties of Strain less steel and Silicon nitrate[10]

Metal:	SUS304	Ceramic:	Si_3N_4
E(Gpa):	207.78×10^9	E(Gpa):	322.27×10^9
μ:	0.3177	μ:	0.24
ρ(kg/m³):	8166	ρ(kg/m³):	2370

4.1 Convergence test

The convergence study of the present model analyzed to determine the uniform mesh size at which the natural frequencies converge and a suitable number of homogeneous layers to represent the FG Spherical panel. In the following, as a first part, to examine the present solution, the convergence properties of the fundamental frequency SUS304/ Si3N4 for spherical shells in the rectangular form with simply supported conditions considered. The results are In Fig.8. The discussion is made only on the present numerical results for the uniform mesh size of 6×6. Therefore, based on the above analysis, the subsequent investigations are carried out using a uniform mesh size of 6×6.

4.2 Comparison Study

Table II. shows the frequencies of the first five modes for a Simply- supported, spherical shell (Rx = Ry = R) in rectangular form. Composed of Aluminum (Al) and Silicon Carbide (Sic) for four different values of the thickness ratios (a/h = 5,20,50, and 200).The power-law distribution parameters FGM (u=1, v=0, w=2, φ=2), Geometrical parameters R/a=5, a/b=1 and five skew angle 0^0, 15^0, 30^0, 45^0, 60^0 are considered. The results of good agreement with the HSDT accurate solutions given by Mouli et al. [26] The maximum difference between them is 1.82% and by using the customized computer code in the MATLAB environment, which is developed based on HSDT formulated by the finite element approach. Some numerical examples solved to show the effectiveness of the present developed model.

4.3 Numerical examples and results

In this section, the FV behavior of the FG spherical shell, which is composed of two constituents ceramic- rich (silicon nitride Si3N4), and metal-rich (stainless steel SUS304), and the material properties same for all numerical examples, and the Poisson's ratios (μ) of both materials 0.3 chosen. The results were analyzed using four-parameter power-law distribution. The material distribution applied through-thickness(ξ) direction. Power-law Variation and choice of power-law material distribution parameters (u, v, w). Examine the influence of the vibration behavior of the FG spherical shell with the effects of the material composition in terms of volume fraction. Four power-law distribution parameters FGM (u, v, w, φ) as in (3) and the significance of geometrical ratios, and skew angle on the non-dimensional frequency responses are FGM structure presented.

Table- II. shows the comparison of Non-dimensional frequency parameter for FG spherical (Aluminum (Al) and Silicon Carbide (Sic)), shell panels with different Thickness (a/h) ratios.

Skew angle(α)											
0^0				15^0		30^0		45^0		60^0	
a/h	Mode	Mouli et.al [26]	Present	Mouli et.al [26]	Present	Mouli et.al [26]	Present	Mouli et.al [26]	Present	Mouli et.al [26]	Present

5	1	3.4100	3.4723	6.8281	6.7500	6.8290	6.7509	7.4322	7.5446	7.4328	7.5452
	2	3.6408	3.7063	7.0037	6.9254	7.0591	6.9807	7.3561	7.4637	8.2882	8.4083
	3	4.4156	4.4915	7.6278	7.5454	7.7858	7.7095	8.0807	8.1815	10.1929	10.3287
	4	6.1069	6.2049	8.9230	8.8249	9.3418	9.2572	9.9786	10.0878	11.8894	11.7596
	5	10.0314	10.1768	11.6240	11.4933	12.7402	12.6242	14.4919	14.5521	14.7162	14.6343
20	1	4.6859	4.7087	9.8392	9.8906	9.8399	9.8913	15.1368	15.2157	19.2254	19.3233
	2	5.2709	5.2962	10.1067	10.1585	11.6470	11.7064	15.8461	15.9268	20.6338	20.7377
	3	6.6948	6.7273	11.8048	11.8646	15.7501	15.8288	18.1545	18.2445	25.3188	25.4429
	4	9.5462	9.5934	15.6993	15.7782	23.3829	23.4959	23.9133	24.0316	32.7678	32.9211
	5	17.1977	17.2814	26.1756	26.3045	37.2351	37.4083	44.4248	44.6480	47.0353	46.9039
50	1	7.9556	7.9688	11.9952	12.0188	11.9964	12.0200	16.9843	17.0197	21.5536	21.5990
	2	8.8234	8.8384	12.8408	12.8659	15.2141	15.2436	19.1813	19.2201	23.5513	23.6006
	3	10.0229	10.0410	14.7504	14.7800	19.9778	20.0184	22.5151	22.5611	29.7915	29.8538
	4	12.7876	12.8121	19.3674	19.4070	29.6364	29.6978	29.9588	30.0198	44.0315	44.1225
	5	21.6786	21.7218	33.2335	33.3015	51.2778	51.3790	56.5794	56.6961	75.5599	75.7033
200	1	28.2112	28.2218	29.7181	29.7298	29.7252	29.7368	32.0759	32.0892	35.0713	35.0865
	2	28.7029	28.7137	30.3673	30.3793	32.3829	32.3963	34.6465	34.6614	36.9586	36.9751
	3	29.1911	29.2023	31.2642	31.2769	34.8612	34.8764	36.6680	36.6830	41.9366	41.9563
	4	30.6427	30.6547	34.2175	34.2323	42.4027	42.4227	43.4188	43.4394	55.7493	55.7774
	5	36.8841	36.9000	47.0289	47.0518	69.3334	69.3690	70.5579	70.5947	101.8152	101.8692

4.3.1 Example

Table III. shows the effect of general boundary conditions, namely- supported (SSSS), clamped boundary condition (CCCC), and Hinged (HHHH) all sides and FGM Power-law distribution(u=1/v=1/w=2/φ=2) and the following geometric values used for the analysis (a/h=10, R/a=5). The results reveal the SSSS condition exhibit lower frequencies for all six modes compared to other boundary conditions. Clamped boundary conditions would also strengthen for all frequency responses. Consequently, it induces higher frequency responses of vibration of the shell. A similar trend mirrored for all the other cases.

Table-III: Variation of non-dimensional frequency responses With (α) for FG spherical shell (SUS304/Si3N4) panel for different boundary conditions.

		Skew angle (α)				
BCC	Mode	0^0	15^0	30^0	45^0	60^0
SSSS	1	6.6053	7.1838	9.0387	13.0503	22.9678
	2	15.1406	15.0826	17.0006	21.9219	34.2981
	3	15.1419	17.2313	22.0854	27.0449	35.4864
	4	20.5923	21.1368	23.0593	28.4055	39.1695
	5	20.5951	21.3085	23.5884	31.0722	45.2798
	6	23.0281	23.3723	25.4397	32.1331	45.6577
CCCC	1	11.1883	11.7655	13.8032	18.6021	30.6740
	2	20.7881	20.6460	22.6770	28.2155	42.2235
	3	20.7881	22.9958	28.1145	37.8034	53.7746
	4	29.0141	29.4013	31.6162	38.7717	58.9064
	5	34.7061	36.2572	40.9409	46.1865	63.2556
	6	35.0660	37.6715	41.5800	48.5456	66.5826
HHHH	1	7.0277	7.5702	9.3421	13.2590	23.0909
	2	15.1740	15.1275	17.0526	21.9776	34.3717
	3	15.1752	17.2516	22.1042	31.1155	45.5663
	4	23.0613	23.4081	25.4796	32.1119	55.4464
	5	28.3663	29.9099	35.1487	41.5272	56.5141
	6	28.3730	31.0243	35.3998	44.7038	58.4264

4.3.2 Example

The effect of curvature ratio (R/a), on the variation of the non-dimensional frequency parameter with four-parameter power-law distribution FGM (u=1/v=0/w=0/φ=5) and FG spherical shell made of SUS304/Si3N4, is described with SSSS CCCC, and HHHH boundary conditions**.**

In Tables IV-VI, respectively the frequency response shown in these three tables. For the above cases, five different values of curvature ratio (R/a = 5,10, 20 and 50,100) and Skew angle range from 0^0 to 60^0 are considered.

Tables IV and V show the frequencies for the first six modes for simply supported and clamped boundary conditions (a/h=10, a/b=1), respectively.it is observed that the natural frequencies in all six modes increase with rising the skew angle. Whereas for shells with curvature ratio grows resultant shell stiffness change, the natural frequencies rates gradually dropped. Although the curvature ratio of any curved shell panel increases consistent approaches to the flatness.

Table VI. shows the non-dimensional frequency rate of the first six modes observed for accelerating trend HHHH boundary condition, with rising skew angle. Descent flow of non-dimensional frequency parameters while increasing curvature ratios.

4.3.3 Example

Tables VII to IX illustrate the effect of the aspect ratio on the frequency responses of the FG spherical shell panel has analyzed. for three different boundary conditions, and following geometric quantiles are five different values of aspect ratio (*a/b* =1, 1.5, 2, 2.5, 3) and the a/h=5, R/a=5 and power-law distribution FGM (u=1/v=1/w=2/φ=2) with five skew angle 0^0,15^0,30^0,45^0,60^0.

The detailed numerical results depicted in Table VII to IX. describe the variation of the fundamental natural frequencies with the power-law distribution, Skew angles for under different boundary conditions, the trend can be seen in numerical results that the non-dimensional frequencies rate slowly improves as the skew angle increases from 0^0 to 30^0.

Pronounced frequency increments occurring when the skew angle rises from 30^0 to 60^0. The result shows that the frequency parameter values are increasing with the aspect ratio. Because the large aspect ratios are comparatively stiffer, and it also prominent affect the structural design and vibration behavior of the structure.

Tables VIII and IX. illustrate the first six frequency modes for Variation of Non-dimensional frequency parameter for clamped condition and hinged condition. The frequencies gradually increase as the aspect ratio increases. Between them CCCC boundary condition exhibit higher frequency parameter values compared to the other boundary condition.

4.3.4 Example

Tables X to XII demonstrates the effect of the thickness ratio on the frequency responses of the FG spherical shell SUS304/Si3N4 panel. With FGM (u=1/v=0/w=2/ φ=2) the following geometric parameters (a/b=1, R/a=5) and different thickness ratio values of (a/h=5,10,20,50,100,200) are presented. Increase the skew angle from 0^0 to 60^0, the interval of 15^0 under three different boundary conditions considered.

Table X shows the frequencies in the first six modes for simply supported with the power-law distribution. The frequency parameters are showing the enhancing type of behavior with the increasing thickness ratio and skew angle. The trends of nondimensional frequency response attributed gradually intensify the first mode to the sixth mode. When the calculations performed with skew angle 0^0 to 60^0.generally, the maximum frequency responses occurred at 60^0. in which the without skew angle 0^0 represents a rectangular spherical shell. The response of the frequency parameter for the skew angle with the thickness ratio increases the rate of stability for all the FGM skew structures.

Table XI and XII shows similar approach the effect of thickness ratio increases with skew angle and power law distribution parameters kept constant non dimensional frequency parameter responses shown for clamped and hinged boundary condition. Increment trends noticed at skew angle more than 30^0.

Table-IV, V and VI: Variation of non-dimensional frequency responses with skew angle (α) for FG spherical shell (SUS304/Si3N4) panel for different curvature ratios(R/a).

Table-IV: (R/a) ratios under SSSS boundary condition

R/a	Mode	0^0	15^0	30^0	45^0	60^0
5	1	8.1342	8.8455	11.1265	16.0583	28.2408
	2	18.6354	18.5634	20.919	26.9614	42.1294
	3	18.6371	21.2048	27.1647	33.3529	43.7535
	4	25.4005	26.0718	28.4416	35.0249	48.2873
	5	25.4039	26.2838	29.0977	38.1963	55.6096
	6	28.329	28.751	31.2875	39.5096	56.2522
10	1	7.852	8.5889	10.9303	15.9359	28.1964
	2	18.54	18.4677	20.8429	26.9226	42.1646
	3	18.5416	21.1294	27.1325	33.3257	43.704
	4	25.3819	26.0521	28.4192	35.0052	48.2337
	5	25.3853	26.2626	29.0588	38.188	55.7096
	6	28.286	28.7097	31.2562	39.484	56.134
20	1	7.7809	8.5248	10.8825	15.9081	28.1906
	2	18.5194	18.447	20.8277	26.918	42.184
	3	18.521	21.1142	27.1297	33.3126	43.6821
	4	25.3726	26.0424	28.4084	34.9941	48.21
	5	25.376	26.2524	29.0431	38.1929	55.7586
	6	28.28	28.7043	31.2538	39.4836	56.0804
50	1	7.7618	8.5078	10.8705	15.9022	28.1924
	2	18.5157	18.4433	20.8259	26.9201	42.1961
	3	18.5173	21.1124	27.1323	33.305	43.67
	4	25.367	26.0366	28.4019	34.9871	48.1968
	5	25.3704	26.2464	29.0349	38.1988	55.7858
	6	28.2815	28.7059	31.2567	39.4873	56.0519
100	1	7.7594	8.5058	10.8692	15.9021	28.1939
	2	18.5159	18.4436	20.8265	26.9215	42.2002
	3	18.5175	21.113	27.1339	33.3025	43.6661
	4	25.3651	26.0347	28.3998	34.9847	48.1925
	5	25.3686	26.2445	29.0324	38.2013	55.7941
	6	28.2828	28.7073	31.2584	39.4892	56.0433

Table-V: (R/a) ratios under CCCC boundary condition

R/a	Mode	0^0	15^0	30^0	45^0	60^0
5	1	13.7852	14.4958	17.0038	22.9074	37.7452
	2	25.5709	25.3974	27.8927	34.6932	51.8779
	3	25.5709	28.2801	34.5590	46.4707	66.0626
	4	35.6781	36.1550	38.8760	47.6140	72.5375
	5	42.6532	44.5548	50.3726	56.8799	77.5000
	6	43.1177	46.3126	51.0773	59.7193	81.8035
10	1	13.4253	14.1547	16.7163	22.6985	37.6241
	2	25.5091	25.3276	27.8275	34.6463	51.8646
	3	25.5091	28.2381	34.5472	46.4393	66.0542
	4	35.6406	36.1137	38.8344	47.6463	72.4524
	5	42.6497	44.5559	50.4235	56.8535	77.6167
	6	43.0799	46.2858	51.0933	59.6466	81.7925
20	1	13.3344	14.0689	16.6446	22.6473	37.5958
	2	25.4983	25.3145	27.8159	34.6402	51.8695
	3	25.4983	28.2329	34.5514	46.4377	66.0605
	4	35.6369	36.1089	38.8297	47.6655	72.4136
	5	42.6568	44.5645	50.4383	56.8378	77.6706
	6	43.0762	46.2856	51.1071	59.6299	81.7971
50	1	13.3094	14.0453	16.6251	22.6338	37.5892
	2	25.4983	25.3137	27.8157	34.6421	51.8761
	3	25.4983	28.2350	34.5572	46.4414	66.0676
	4	35.6396	36.1112	38.8320	47.6780	72.3915
	5	42.6638	44.5723	50.4424	56.8276	77.7015
	6	43.0789	46.2896	51.1173	59.6262	81.8030
100	1	13.3060	14.0422	16.6226	22.6322	37.5887
	2	25.4994	25.3146	27.8167	34.6437	51.8789
	3	25.4994	28.2365	34.5596	46.4434	66.0705
	4	35.6413	36.1128	38.8336	47.6824	72.3844
	5	42.6666	44.5753	50.4429	56.8240	77.7115
	6	43.0806	46.2916	51.1210	59.6260	81.8056

Table-VI: (R/a) ratios under HHHH boundary condition

R/a	Mode	0^0	15^0	30^0	45^0	60^0
5	1	8.4725	9.1523	11.3585	16.2029	28.3116
	2	18.6498	18.5873	20.9517	27.0024	42.2158

Table-VII: (a/b) ratios under SSSS boundary condition

a/b	Mode	0^0	15^0	30^0	45^0	60^0
5	1	5.7832	6.1551	7.4093	10.1490	16.4495
	2	10.2960	10.5675	11.5274	13.5194	17.7337

	3	18.6514	21.2125	27.1854	38.2220	55.9456
	4	28.3367	28.7615	31.3040	39.4841	68.1196
	5	34.8603	36.7765	43.2093	51.0223	69.4244
	6	34.8888	38.1261	43.5059	54.9756	71.7047
10	1	7.9025	8.6339	10.9621	15.9529	28.2036
	2	18.5404	18.4693	20.8465	26.9288	42.1888
	3	18.5420	21.1300	27.1396	38.1926	55.9460
	4	28.2863	28.7103	31.2579	39.4785	68.1538
	5	34.8334	36.7561	43.2031	51.0244	69.3626
	6	34.8634	38.1083	43.4965	54.9021	71.7217
20	1	7.7825	8.5262	10.8835	15.9093	28.1944
	2	18.5205	18.4478	20.8286	26.9197	42.1931
	3	18.5221	21.1161	27.1342	38.1968	55.9594
	4	28.2842	28.7082	31.2574	39.4832	68.1664
	5	34.8369	36.7576	43.2085	51.0342	69.3353
	6	34.8635	38.1141	43.5028	54.8753	71.7419
50	1	7.7673	8.5132	10.8761	15.9096	28.2032
	2	18.5198	18.4470	20.8291	26.9231	42.2013
	3	18.5213	21.1165	27.1367	38.2054	55.9717
	4	28.2905	28.7145	31.2643	39.4884	68.1723
	5	34.8444	36.7623	43.2145	51.0428	69.3204
	6	34.8677	38.1222	43.5102	54.8625	71.7577
100	1	7.7718	8.5175	10.8803	15.9141	28.2085
	2	18.5214	18.4488	20.8312	26.9257	42.2049
	3	18.5230	21.1181	27.1384	38.2093	55.9765
	4	28.2938	28.7178	31.2678	39.4906	68.1741
	5	34.8478	36.7644	43.2169	51.0462	69.3156
	6	34.8697	38.1257	43.5132	54.8588	71.7635

	3	10.2974	10.6524	11.7823	14.1991	19.5705
	4	12.4627	12.3156	13.4380	16.4416	22.7025
	5	12.4637	13.8485	15.9620	18.1586	23.5558
	6	14.6075	14.9162	16.9025	22.1652	29.7113
10	1	8.7493	9.2233	10.8367	13.0822	16.1514
	2	10.3129	10.5758	11.4255	14.4034	22.7390
	3	14.8484	15.3831	17.1976	20.9389	28.4447
	4	15.4680	15.9442	17.5393	21.1489	28.5110
	5	18.6116	18.9673	20.1997	22.8512	30.0434
	6	20.6398	21.1333	22.7244	25.9653	32.8987
20	1	10.3194	10.5320	11.2000	12.4246	14.4644
	2	12.4448	13.0797	15.2538	20.0984	28.7650
	3	17.9209	18.5898	20.8499	24.2538	31.4612
	4	20.6370	20.9460	21.9990	25.7646	36.9860
	5	20.6530	21.2952	23.5075	28.2407	38.2955
	6	23.0793	23.7602	25.9268	30.3184	39.7546
50	1	10.3226	10.4999	11.0476	12.0192	13.5621
	2	16.6249	17.4449	20.2535	23.8835	27.4354
	3	20.6595	20.9632	21.9543	26.5005	41.0208
	4	21.5121	22.3313	25.1120	31.2112	41.6013
	5	25.8039	26.6442	29.4697	34.9583	45.2808
	6	27.7910	28.5880	31.2314	35.7258	48.8631
100	1	10.3244	10.4767	10.9425	11.7546	13.0166
	2	20.6632	20.9428	21.8322	23.4993	26.4443
	3	21.1191	22.1321	25.5951	33.2566	40.9791
	4	25.4832	26.4711	29.8332	35.2322	50.5276
	5	30.9693	31.4171	32.6128	37.2392	50.9167
	6	31.0842	31.9940	35.4394	42.8158	54.3551

Table-VII, VIII and IX: Variation of non-dimensional frequency responses with skew angle (α) for FG spherical shell (SUS304/Si3N4) panel for different aspect ratios(a/b).

Table-VIII: (a/b) ratios under CCCC boundary condition

a/b	Mode	0^0	15^0	30^0	45^0	60^0
5	1	8.8081	9.2064	10.5665	13.5559	20.3344
	2	15.1719	15.0371	16.1793	19.2491	26.5813
	3	15.1719	16.5252	19.4987	23.1289	29.4766
	4	19.9190	19.6581	20.5361	24.8215	32.8185
	5	19.9190	20.5161	21.6284	25.3180	37.8290
	6	20.3675	21.2588	24.0197	29.2839	39.4421
10	1	12.7704	13.3237	15.2007	19.2854	28.4888
	2	17.9687	18.5113	20.3743	24.4824	33.8373
	3	22.9911	23.4205	24.9741	28.5828	37.0965
	4	24.0548	25.1109	27.3669	31.4131	41.2999
	5	25.5670	25.8417	28.6288	35.9897	48.6611
	6	27.6275	28.6193	31.8757	38.6576	49.0154
20	1	17.4387	18.1694	20.6443	26.0239	38.1852
	2	21.6496	22.3581	24.7632	30.0128	41.9662
	3	26.7273	27.3531	29.5185	34.3773	45.7153
	4	28.3553	29.0063	31.2859	36.4409	48.5104
	5	33.2734	34.5870	38.5906	44.2202	56.1039
	6	35.8010	37.0181	39.8496	45.5064	57.0656
50	1	22.3722	23.2845	26.3739	33.0956	48.3317
	2	25.8568	26.7354	29.7175	36.2373	51.1426
	3	30.8821	31.6926	34.4757	40.6673	55.0277
	4	31.7374	32.5695	35.4204	41.7420	56.4424
	5	39.5202	40.2735	42.9838	49.2693	63.8587
	6	42.4532	43.0424	45.3010	50.7194	64.3654
100	1	27.4183	28.5139	32.2258	40.3106	58.6562
	2	30.3728	31.4296	35.0188	42.8773	60.8623
	3	35.3061	36.3030	39.7150	47.2690	64.6982
	4	35.5511	36.5563	39.9883	47.5752	65.1883
	5	42.6764	43.6347	46.9519	54.4237	72.1211
	6	45.8049	46.6176	49.5032	56.1805	72.2195

Table-IX: (a/b) ratios under HHHH boundary condition

a/b	Mode	0^0	15^0	30^0	45^0	60^0
5	1	5.9072	6.2717	7.5068	10.2225	16.5003
	2	12.4582	12.3155	13.4385	16.4407	23.5516
	3	12.4592	13.8363	16.8789	21.4710	27.0510
	4	17.9300	18.0399	19.0909	22.1785	29.8667
	5	18.4713	18.2926	19.1250	22.8874	34.8976
	6	18.4714	19.5931	21.9185	26.2786	36.2695
10	1	8.8343	9.3043	10.9069	14.4586	22.7780
	2	14.8595	15.3941	17.2089	21.1565	30.0536
	3	21.0959	22.0483	23.5298	26.9530	35.0236
	4	21.6577	22.1776	24.8005	28.7235	38.2320
	5	23.1498	23.3571	25.7373	32.2356	41.9301
	6	24.3454	25.1272	27.6398	33.6465	43.7713
20	1	12.5078	13.1401	15.3069	20.1412	31.4891
	2	17.9394	18.6082	20.8683	25.7830	37.0051
	3	25.5191	26.1277	28.2378	32.9834	44.0814
	4	25.6167	26.2474	28.4495	33.3947	44.8479
	5	29.6972	30.6271	33.4890	39.0482	49.4467
	6	30.9413	32.2413	36.2565	41.3063	50.9772
50	1	16.6747	17.4928	20.2963	26.5338	41.0442
	2	21.5333	22.3523	25.1325	31.2312	45.2959
	3	28.5877	29.3856	32.1067	38.1001	50.6459
	4	29.7861	30.5863	33.3363	39.4611	51.9090
	5	35.1859	36.1327	39.1974	45.2062	53.6732
	6	37.1813	37.8976	40.4914	46.4918	55.8732
100	1	21.1603	22.1716	25.6301	33.2848	50.5074
	2	25.5048	26.4925	29.8540	37.2561	50.9363
	3	31.9658	32.9208	36.1718	43.3341	54.3695
	4	34.3046	35.2955	38.6883	46.2018	55.2704
	5	40.0165	40.9343	44.1032	49.9764	60.0647
	6	40.0737	41.0880	44.3515	50.8968	61.3982

International Journal of Engineering and Advanced Technology (IJEAT)
ISSN: 2249 – 8958, Volume-9 Issue-3, February, 2020

Table-X, XI and XII: Variation of non-dimensional frequency responses with skew angle (α) for FG spherical shell (SUS304/Si3N4) panel for different thickness ratios(a/h).

Table-X:(a/h) ratios under SSSS boundary condition

a/h	Mode	0^0	15^0	30^0	45^0	60^0
5	1	6.4517	6.8699	8.2806	11.3646	18.4674
	2	11.6504	11.9565	13.0387	15.2824	20.0147
	3	11.6520	12.0521	13.3247	16.0424	22.0580
	4	13.9565	13.7928	15.0633	18.4601	25.5604
	5	13.9576	15.5193	18.0279	20.4892	26.5075
	6	16.5076	16.8543	18.9669	24.9091	33.2308
10	1	7.3587	8.0082	10.0863	14.5776	25.7048
	2	16.8844	16.8245	18.9806	24.5054	38.4166
	3	16.8859	19.2291	24.6798	30.5808	40.1139
	4	23.2894	23.9049	26.0777	32.1123	44.2728
	5	23.2926	24.0993	26.6772	34.7869	50.8794
	6	25.7174	26.1095	28.4429	35.9860	51.5037
20	1	8.6163	9.6496	12.3159	17.7039	31.9963
	2	18.5522	18.9439	22.0618	29.3192	48.7200
	3	18.5535	21.8058	29.3455	43.4518	68.7196
	4	28.6498	29.7997	33.8983	44.5543	80.1802
	5	36.3118	38.8862	47.4876	60.5394	82.5620
	6	36.3335	40.8847	48.7292	61.2053	88.6178
50	1	13.9863	15.6158	18.0300	23.4077	40.2479
	2	22.0573	23.5621	27.2538	35.9980	61.7974
	3	22.0593	27.8375	37.0190	55.2876	94.6650
	4	31.7649	35.5501	41.8746	55.6843	105.5847
	5	40.4874	44.1676	55.8575	81.8853	138.3160
	6	40.5048	50.8533	61.1467	82.4093	153.6224
100	1	25.0060	26.4585	28.0029	32.2984	48.5788
	2	30.3975	32.1713	35.1455	43.4712	72.0867
	3	30.4025	37.3366	44.9454	63.1893	113.6363
	4	38.1385	43.7978	49.4988	64.8212	119.2980
	5	46.1670	50.4299	62.4724	91.5951	173.9507
	6	46.2108	60.4894	70.1668	96.1937	176.2264
200	1	48.4058	49.3974	50.3769	53.3064	65.8688
	2	51.5289	52.8462	54.7069	60.7414	86.1456
	3	51.5408	56.9300	62.0211	77.0992	129.1362
	4	56.4229	61.5382	65.6368	79.0476	131.7246
	5	62.4662	66.2262	76.1777	103.2203	191.4092
	6	62.5921	75.3887	83.7672	109.7436	197.5931

Table-XI:(a/h) ratios under CCCC boundary condition

a/h	Mode	0^0	15^0	30^0	45^0	60^0
5	1	9.8794	10.3289	11.8646	15.2442	22.9182
	2	17.0054	16.8584	18.1480	21.6055	29.8225
	3	17.0054	18.5208	21.8475	26.1381	33.2650
	4	22.5459	22.2448	23.2275	27.9311	36.9571
	5	22.5459	23.0560	24.3189	28.3150	41.8291
	6	22.8831	24.0663	27.1979	33.1954	44.4823
10	1	12.4969	13.1428	15.4252	20.8108	34.4046
	2	23.2365	23.0804	25.3660	31.6018	47.4040
	3	23.2365	25.7121	31.4611	42.4077	60.4605
	4	32.4781	32.9189	35.4217	43.4496	66.5092
	5	38.8871	40.6343	46.1443	52.1455	71.0082
	6	39.3024	42.2337	46.6325	54.5972	74.9676
20	1	14.7733	15.4882	18.0953	24.6611	43.2079
	2	27.3522	27.2829	30.4831	39.4002	63.8952
	3	27.3522	30.4735	38.1045	55.1545	86.1917
	4	39.2357	40.1434	44.2924	55.5490	99.1637
	5	49.0480	51.6557	60.7964	75.1619	112.5701
	6	49.4081	53.3924	61.7315	82.1526	133.1525
50	1	21.6519	22.2498	24.5787	31.1803	52.6386
	2	32.1869	32.4095	36.6455	48.6762	83.6657
	3	32.1869	35.5488	44.4434	65.6432	123.1431
	4	45.3456	47.1128	54.1330	72.5531	125.0019
	5	58.6460	62.2989	75.3989	105.7419	175.1750
	6	59.1405	63.9297	79.6030	107.1998	192.3387
100	1	35.8385	36.2717	38.0129	43.3448	63.6282
	2	39.8495	40.3595	44.7236	57.5701	98.5983
	3	39.8495	42.6585	51.0047	72.8823	139.4303
	4	51.7569	53.8672	62.0961	84.5981	151.6135
	5	65.0468	68.9822	83.5305	120.8450	228.1453
	6	66.3525	71.1334	88.5242	126.4352	228.7171
200	1	60.2444	61.2051	65.1993	72.2223	88.1821
	2	60.2444	61.7507	67.3210	76.5853	116.4895
	3	64.4821	65.0573	67.6684	86.0960	151.9361
	4	68.9093	71.2773	79.1972	100.7317	173.5670
	5	79.0675	82.5304	95.8739	132.7832	249.6854
	6	85.1334	88.4739	102.6578	142.6604	265.1871

Table-XII:(a/h) ratios under HHHH boundary condition

a/h	Mode	0	150	300	450	600
	1	6.5043	6.9184	8.3188	11.3914	18.4895
	2	13.9562	13.7929	15.0597	18.4501	26.485
	3	13.9574	15.5164	18.9606	24.1052	30.2169
	4	20.1151	20.2391	21.4272	24.9177	33.6033
	5	20.7755	20.5796	21.5076	25.7742	38.5514
5	6	20.7755	22.0166	24.578	29.3184	40.7274
	1	7.6274	8.2508	10.2663	14.6839	25.75
	2	16.8923	16.8397	19.0029	24.5347	38.4816
	3	16.8937	19.2333	24.697	34.8032	51.1046
	4	25.7194	26.1136	28.4516	35.9653	62.2911
	5	31.6884	33.4479	39.3525	46.5531	63.6993
10	6	31.7164	34.6827	39.6279	50.4194	65.62
	1	9.8126	10.715	13.1239	18.2154	32.2128
	2	18.6299	19.0468	22.1707	29.4154	48.7839
	3	18.6309	21.8534	29.375	43.4947	68.751
	4	28.6833	29.8391	33.9445	44.5793	82.6698
	5	36.3233	38.8906	47.4931	60.622	93.1407
20	6	36.3377	40.8951	48.7465	66.8741	115.9704
	1	19.0081	20.0154	21.7918	26.313	41.8617
	2	22.7683	24.2892	27.9856	36.6878	62.2776
	3	22.7685	28.3149	37.3185	55.456	94.888
	4	32.2559	36.0186	42.3101	56.0477	105.6741
50	5	40.6212	44.3109	55.9463	82.0314	138.406
	6	40.7725	51.0893	61.3167	82.4648	153.6792
	1	32.7629	34.3303	37.1176	40.5725	54.3817
	2	32.763	35.9367	37.5206	46.0223	74.1566
	3	35.5695	38.9013	46.0622	63.8692	114.6493
	4	40.2672	45.6218	51.2829	66.3641	119.6135
	5	46.8356	51.3067	63.0039	91.8995	174.3796
100	6	48.277	61.2964	70.9567	96.8843	176.3885
	1	57.0694	57.8103	60.4599	68.0053	82.6111
	2	57.0695	60.8844	65.4804	71.4613	93.7315
	3	60.1267	62.3732	65.6316	79.5537	132.8953
	4	62.6182	67.3913	73.5671	85.3047	133.4042
	5	64.7978	72.0147	78.9201	104.6425	192.0976
200	6	73.2334	78.3517	86.9426	112.7345	199.6014

HSDT conjunction with the finite element method. The comparison studies divulge the accuracy of the current model, and good agreement observed those available in the literature. The results computed via MATLAB environment.to show the robustness of the formulation explores different sets of geometrical parameters of the shell curvature ratio, aspect ratio, and thickness ratio, and choice of material distribution parameters, and skew angles under various boundary conditions considered here.

Based on the parametric study, numerical results revealed by using the four-parameter Power-law distribution on rectangular spherical shell and influence of u, v, and w parameters on the non-dimensional frequency responses examined. The following important conclusion from this study is summarized.

- The frequency responses are decreasing trend as the curvature ratio increases.
- The frequency responses are gradually rising as the thickness ratio and aspect ratio increases.
- In all cases, the boundary conditions have a perceptible effect on the frequency parameter of the spherical shell. The frequency parameters are higher for all the FG shell clamped boundary conditions.
- Variation of frequency parameter with a different power-law exponent (φ) and material parameters (u, v, and w) It is possible to approach to change the behavior of the structure.

- The influence of skewangles the non-dimensional frequency parameters exhibit 00 for minimum at 600 maximum response. all the frequency parameter values are escalating with skewangles.
- The frequency responses are maximum and minimum for the spherical shells.

V. SUMMARY AND CONCLUSIONS

In this study, free vibration responses of FGM spherical shell (SUS304/(Si3N4) rectangular form observed and presented. The FGM material composition, material properties vary continuously from metal (top/bottom surface) to ceramic (base/top surface). Employed Voigt's micromechanical model achieved through the four-parameter power-law distribution of the volume fractions. Convergence and comparison tests performed to illustrate the stability and exactness of the present mathematical model governed by

REFERENCES

1. C. T. Loy, K. Y. Lam, and J. N. Reddy, "Vibration of functionally graded cylindrical shells," *Int. J. Mech. Sci.*, vol. 41, no. 3, pp. 309–324, 1999.
2. S. C. Pradhan, C. T. Loy, K. Y. Lam, and J. N. Reddy, "Vibration characteristics of functionally graded cylindrical shells under various boundary conditions," vol. 61, pp. 111–129, 2000.
3. J.N.Reddy, "Analysis of functionally graded plates," *Int. J. Numer. Methods Eng.*, vol. 47, no. June 1999, pp. 663–684, 2000. 4.T. Y. Ng, K. Y. Lam, K. M. Liew, and J. N. Reddy, "Dynamic stability analysis of functionally graded cylindrical shells under periodic axial loading," *Int. J. Solids Struct.*, vol. 38, no. 8, pp. 1295–1309, 2001.
5. K. M. Liew, L. X. Peng, and T. Y. Ng, "Three-dimensional vibration analysis of spherical shell panels subjected to different boundary conditions," vol. 44, pp. 2103–2117, 2002.
6. J. N. Reddy and Z. Cheng, "Frequency correspondence between membranes and functionally graded spherical shallow shells of polygonal planform," vol. 44, pp. 967–985, 2002.
7. X. X. Hu, T. Sakiyama, H. Matsuda, and C. Morita, "Vibration analysis of rotating twisted and open conical shells," *Int. J. Solids Struct.*, vol. 39, no. 25, pp. 6121–6134, 2002.
8. E. Artioli and E. Viola, "Free vibration analysis of spherical caps using a G.D.Q. numerical solution," *J. Press. Vessel Technol. Trans. ASME*, vol. 128, no. 3, pp. 370–378, 2006.
9. R. A. Arciniega and J. N. Reddy, "Large deformation analysis of functionally graded shells," *Int. J. Solids Struct.*, vol. 44, no. 6, pp. 2036–2052, 2007.
10. X. Zhao, Y. Y. Lee, and K. M. Liew, "Free vibration analysis of functionally graded plates using the element-free kp-Ritz method," *J. Sound Vib.*, vol. 319, no. 3–5, pp. 918–939, 2009.
11. F. Tornabene and E. Viola, "Vibration analysis of spherical structural elements using the GDQ method," *Comput. Math. with Appl.*, vol. 53, no. 10, pp. 1538–1560, 2007.
12. F. Tornabene and E. Viola, "2-D solution for free vibrations of parabolic shells using generalized differential quadrature method," *Eur. J. Mech. A/Solids*, vol. 27, no. 6, pp. 1001–1025, 2008.
13. F. Tornabene, "Free vibration analysis of functionally graded conical, cylindrical shell and annular plate structures with a four-parameter power-law distribution," *Comput. Methods Appl. Mech. Eng.*, vol. 198, no. 37–40, pp. 2911–2935, 2009.
14. E. Viola and F. Tornabene, "Free vibrations of three parameter functionally graded parabolic panels of revolution," *Mech. Res. Commun.*, vol. 36, no. 5, pp. 587–594, 2009.
15. F. Tornabene and E. Viola, *Free vibrations of four-parameter functionally graded parabolic panels and shells of revolution*, vol. 28, no. 5. 2009.
16. F. Tornabene and A. Ceruti, "Mixed static and dynamic optimization of four-parameter functionally graded completely doubly curved and degenerate shells and panels using GDQ method," *Math. Probl. Eng.*, vol. 2013, 2013.
17. M. H. Yas and B. Sobhani Aragh, "Three-dimensional analysis for thermoelastic response of functionally graded fiber reinforced cylindrical panel," *Compos. Struct.*, vol. 92, no. 10, pp. 2391–2399, 2010.
18. M. Amabili and J. N. Reddy, "A new non-linear higher-order shear deformation theory for large-amplitude vibrations of laminated doubly curved shells," *Int. J. Non. Linear. Mech.*, vol. 45, no. 4, pp. 409–418, 2010.
19. M. Talha and B. N. Singh, "Static response and free vibration analysis of FGM plates using higher order shear deformation theory," *Appl. Math. Model.*, vol. 34, no. 12, pp. 3991–4011, 2010.
20. H. Shen and Z. Wang, "Assessment of Voigt and Mori – Tanaka models for vibration analysis of functionally graded plates," *Compos. Struct.*, vol. 94, no. 7, pp. 2197–2208, 2012.
21. A. M. A. Neves *et al.*, "Free vibration analysis of functionally graded shells by a higher-order shear deformation theory and radial basis functions collocation, accounting for through-the-thickness deformations," *Eur. J. Mech. A/Solids*, vol. 37, pp. 24–34, 2013.
22. S. K. P. Vishesh Ranjan Kar, "Free vibration responses of temperature dependent functionally graded curved panels under thermal environment," pp. 2006–2024, 2015.
23. A. Kumar, A. Chakrabarti, and P. Bhargava, "Vibration analysis of laminated composite skew cylindrical shells using higher order shear deformation theory," *JVC/Journal Vib. Control*, vol. 21, no. 4, pp. 725–735, 2015.
24. C. Zhang, G. Jin, X. Ma, and T. Ye, "Vibration analysis of circular cylindrical double-shell structures under general coupling and end boundary conditions," *Appl. Acoust.*, vol. 110, pp. 176–193, 2016.
25. D. Punera and T. Kant, "Free vibration of functionally graded open cylindrical shells based on several refined higher order displacement models," *Thin-Walled Struct.*, vol. 119, 2017.
26. C. M. Badiganti and R. Koona, "Harmonic frequency analysis of skewed functionally graded flat and spherical shallow shells," *Results Phys.*, vol. 10, no. June, pp. 987–992, 2018.
27. B. C. Mouli, V. R. Kar, K. Ramji, and M. Rajesh, "Free vibration of functionally graded conical shell," *Mater. Today Proc.*, vol. 5, no. 6, pp. 14302–14308, 2018.
28. B. C. Mouli, K. Ramji, V. R. Kar,subrata k panda,lalepalli Anil k and harsh k pandey "Numerial sudy of temperature dependent eigen frequency response of tilted functionally graded shell structures," *structural engineering and mechanics.*, vol. 68, no. 5, pp. 527–536, 2018.
29. Cook, R. D. Malkus, D. S. Plesha, M. E., Witt, R. J., (2009). Concepts and applications of finite element analysis. John Wiley & Sons (Singapore).
30. Pandya, B.N., Kant, T. (1988a). Higher-order shear deformable theories for flexure of sandwich plates-Finite element evaluations. International Journal of Solids and Structures 24(12): 1267-1286.
31. Pandya, B.N., Kant, T. (1988b). Finite element analysis of laminated composite plates using a Higher-order displacement model. Composite Science and Technology 32: 137-155.

AUTHORS PROFILE

Raparthi Srilakshmi, Research Scholar in the Department of Mechanical Engineering, Andhra University has published paper on conditon monitoring. She has Diploma in Polytechnic, BE Mechanical, and M.Tech in Machine Design. She is interested in the areas of FEA, Composites, Solid Mechanics, Vibration Analysis, Signal Analysis, Condition Monitoring and SHM.

Prof. Ch. Ratnam, Professor and Head of the Department in the Department of Mechanical Engineering, Andhra University. He has books published on Fluid Mechanics & Machinery and Geometrical Drawing. He also received an award for best paper published in IEI Journal for the year 2003-2004 and has over 60 papers in National and International journals. He has ample knowledge in Mechanical Engineering and Science, Vibration and Structural Health Monitoring, Engineering Optimization, Finite Element Analysis, Computer Aided Design and Design of Engineering.

Chandra Mouli Badiganti, Assoc. Professor in the Department of Mechanical Engineering of RISE Krishna Sai Prakasam Group of Institution has published around 11 papers in various reputed journals. He has teaching experience in Strength of Materials, Composites,Engineering Drawing, Production Engineering.